Joint Compound-Heat and Chronic-Disease Vulnerability for Geographically Targeting Heat-Resilience Research Grants Across the Contiguous United States

Heat-Resilience Analytics Working Group

Prepared for a heat-resilience research grant prioritization exercise using
Daymet V4 R1 (1991–2020) and CDC PLACES County Data (2024)

July 2026

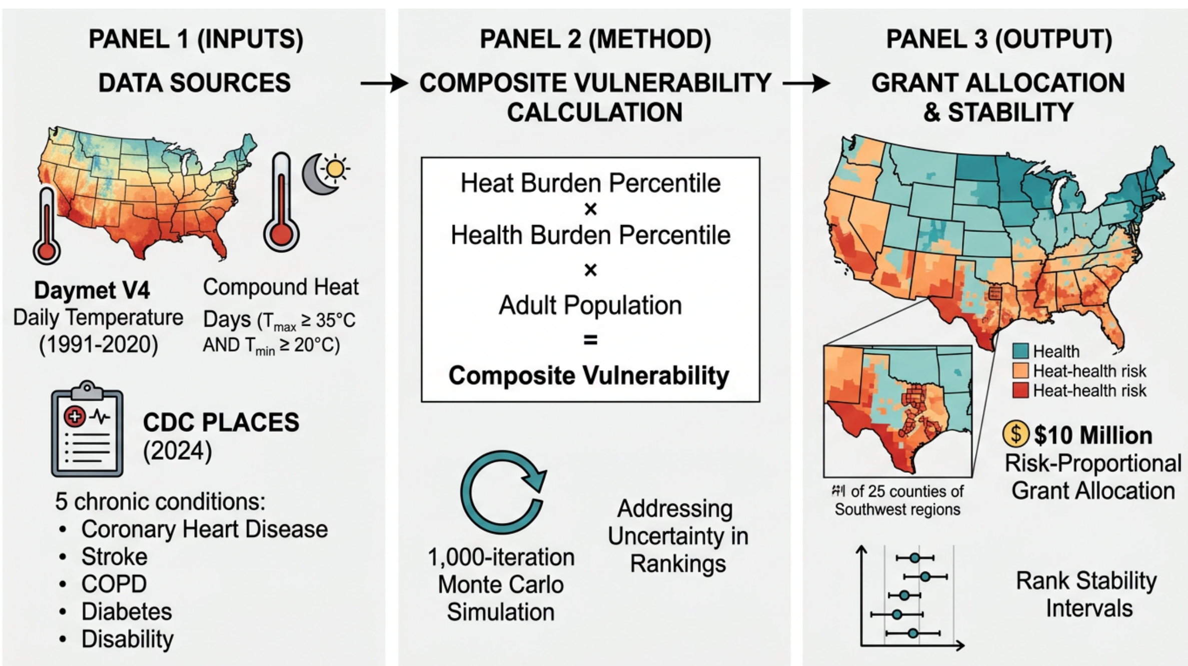

Graphical abstract. A reproducible pipeline joins three decades of Daymet daily temperature with small-area chronic-disease estimates from CDC PLACES. Heat burden (annual days with $T_{\max} \geq 35\,^{\circ}\mathrm{C}$ *and* $T_{\min} \geq 20\,^{\circ}\mathrm{C}$) and health burden (five age-adjusted conditions) are each converted to national percentiles and multiplied by adult population to form a joint composite vulnerability score. A 1,000-iteration Monte Carlo simulation propagates interannual climate variability and PLACES confidence intervals to yield rank-stability intervals, a risk-proportional $10M allocation across 25 recommended counties, and a formal comparison against heat-only and health-only rankings.

Abstract

Extreme heat is the deadliest weather hazard in the United States, and its lethality is concentrated where intense daytime heat coincides with warm nights that block physiological recovery and where populations already carry a heavy burden of heat-sensitive chronic disease. Research and adaptation funding, however, is frequently allocated along a single axis—either climatological hazard or health status—which can misdirect scarce resources. We develop a transparent, fully reproducible framework that jointly ranks all 3,109 contiguous-U.S. counties by *compound* heat exposure, chronic-disease burden, and the size of the population at risk. Using Daymet V4 R1 daily maximum and minimum temperature (1991–2020) aggregated to county centroids, we define a compound heat day as a calendar day with $T_{\max} \geq 35\,^{\circ}\mathrm{C}$ and $T_{\min} \geq 20\,^{\circ}\mathrm{C}$, and we express each county's 30-year mean count as a national percentile. From the CDC PLACES 2024 county file we compute a health-burden percentile as the mean national percentile across five age-adjusted conditions—coronary heart disease, stroke, chronic obstructive pulmonary disease (COPD), diabetes, and disability. A composite vulnerability score is the product of the heat-burden percentile, the health-burden percentile, and the adult population. We propagate interannual climate variability (a 30-year bootstrap) and PLACES sampling uncertainty (Gaussian draws from reported 95% confidence intervals) through 1,000 Monte Carlo iterations, recomputing the full ranking each time to obtain rank-stability intervals and each county's probability of belonging to the top 25. We then design a risk-proportional \$10 million allocation and compare the joint ranking against four single-axis schemes using Jaccard overlap. The recommended 25 counties are strongly clustered in the South and Southwest (21 of 25 in Sun Belt states), led by Harris (TX), Maricopa (AZ), Dallas (TX), Los Angeles (CA), and Bexar (TX); together they contain 43,621,450 adults, roughly one-sixth of the contiguous-U.S. adult population. The ranking is highly stable—24 of 25 counties have a > 0.7 probability of remaining in the top 25 (mean 0.95)—and the risk-proportional allocation ranges from \$1.47 M (Harris) to \$0.21 M (Tulsa). Crucially, the joint index is not reproducible by any single-axis ranking: its top-25 set shares only 0 % of members with a health-only intensity ranking, 9 % with a heat-only intensity ranking, and at most 61 % with a population-weighted health ranking. These results argue for allocating heat-resilience research grants on the basis of *joint* exposure–sensitivity–population burden rather than any single dimension, and they provide a defensible, uncertainty-aware shortlist for programme officers.

Keywords: compound heat extremes; hot nights; chronic disease; heat vulnerability; environmental justice; Monte Carlo; grant allocation; Daymet; CDC PLACES

1 Introduction

Extreme heat is the leading cause of weather-related death in the United States, exceeding the mortality attributable to hurricanes, floods, and tornadoes combined in a typical year [1, 2]. Its public-health footprint is expanding: anthropogenic warming has already increased the frequency, intensity, and duration of heatwaves, and climate models project further intensification through the twenty-first century [3–5]. Because heat kills through the failure of human thermoregulation rather than through mechanical force, its toll is not distributed randomly across the landscape. Instead, it concentrates in places where the climatological hazard is severe, where the built environment amplifies exposure, and where the resident population is physiologically least able to compensate [6, 7]. Understanding *where* these dimensions coincide is a prerequisite for allocating the finite research and adaptation resources that governments and funders can bring to bear.

A central but historically under-appreciated feature of dangerous heat is its *compound* day–night structure. The human body dissipates the heat load accumulated during a hot day primarily at night, when cooler ambient temperatures permit cutaneous and respiratory heat loss and restorative sleep. When nighttime minimum temperatures remain elevated—so-called "hot nights" or "tropical nights"—this recovery window closes, cardiovascular and thermoregulatory strain carries over into the following day, and mortality rises disproportionately [8, 9]. Epidemiological analyses in London, Barcelona, Paris, and Vienna have shown that nighttime heat is an independent predictor of death after accounting for daytime maxima, and that the most lethal episodes are those in which hot days and hot nights occur in succession [8–10]. The catastrophic 1995 Chicago heat wave, in which more than 700 excess deaths occurred over a few days, was characterized precisely by this persistence of heat across the diurnal cycle [11]. Critically, minimum temperatures have been warming faster than maxima over recent decades, so the mortality burden attributable to compound day–night heat is projected to grow even more rapidly than that attributable to daytime extremes alone [12]. Integrated assessments of temperature-related death and illness in the United States likewise project substantial increases in heat-attributable mortality under continued warming, with the largest absolute burdens falling on populous and already-warm regions [13]. Any exposure metric that counts only hot days therefore systematically understates the hazard where recovery is impaired; a metric requiring *both* an extreme daytime maximum and an elevated nighttime minimum on the same calendar day captures the physiologically relevant threat far more faithfully.

The lethality of any given heat exposure is strongly modified by the health status of the exposed population. Thermoregulation depends on an intact cardiovascular system to redistribute blood flow to the skin, on functional kidneys and fluid balance, and on respiratory and metabolic reserve; each of these is compromised in common chronic diseases [14]. People living with cardiovascular disease, including coronary heart disease and prior stroke, face elevated risk because the cardiac output demanded by thermoregulation competes with already limited reserve, and many cardiovascular medications impair sweating or volume regulation [14, 15]. Chronic obstructive pulmonary disease heightens vulnerability through impaired gas exchange and the ventilatory cost of heat dissipation; diabetes blunts autonomic and sweat responses and is associated with dehydration and renal injury under heat stress; and physical disability constrains the behavioural adaptations—seeking shade, operating cooling, relocating—on which survival often depends [14, 16]. A large body of epidemiological evidence confirms that these conditions sharply increase the relative risk of heat-related death and hospitalization [6, 16], and county-level analyses in the United States demonstrate that cardiovascular mortality in particular rises measurably on extreme-heat days [15, 17]. The prevalence of these conditions is highly uneven geographically, following the well-known diagonal band of cardiometabolic disease burden across the American South and Appalachia, so the spatial overlap of heat and chronic disease is neither uniform nor easily predicted from climate alone.

A third dimension—the sheer number of people exposed—determines the aggregate, population-scale burden that policy is ultimately trying to reduce. Two counties with identical hazard and identical disease prevalence do not present identical policy problems if one contains a few thousand adults and the other several million. Large metropolitan counties combine substantial exposed populations with urban-heat-island amplification, in which the built environment elevates both daytime and, especially, nighttime temperatures relative to surrounding rural areas [18, 19]. This urban intensification is itself inequitably distributed: within U.S. cities, historically marginalized and formerly redlined neighbourhoods experience systematically higher surface and air temperatures and possess fewer cooling resources than wealthier, whiter neighbourhoods [20–22]. Population-weighting a vulnerability index therefore does more than maximize the number of beneficiaries; it tends to direct attention toward the dense urban cores where heat, disease, and social disadvantage are most tightly interwoven.

The dominant analytic tradition for prioritizing places has been the construction of composite heat-vulnerability indices, which combine exposure, sensitivity, and adaptive-capacity indicators into a single score [23, 24]. Such indices have proven valuable for within-city and regional planning, but they suffer from two recurrent limitations when used to steer national funding. First, many indices reduce the climate hazard to a coarse or annual-average temperature and neglect the compound day–night structure that governs physiological risk. Second, index scores are typically reported as point estimates, with no accompanying measure of how sensitive a county's rank is to the uncertainty in its inputs—uncertainty that is substantial for both interannual climate variability and for the model-based small-area disease estimates that underpin datasets such as CDC PLACES [25, 26]. A programme officer choosing between the 24th- and 28th-ranked counties deserves to know whether that ordering is robust or an artefact of noise. Best practice in the composite-indicator literature is precisely to propagate input uncertainty through the aggregation and to report the resulting distribution of ranks [27].

In this study we address both limitations directly. We build a joint vulnerability framework that (i) uses a physiologically motivated *compound* heat-exposure metric derived from three decades of high-resolution daily temperature data; (ii) integrates five age-adjusted chronic-disease prevalences from the most recent CDC PLACES release; (iii) weights by the adult population actually at risk; and (iv) rigorously propagates both climatic and epidemiological uncertainty through a Monte Carlo simulation to deliver rank-stability intervals and top-set membership probabilities. We use the framework to recommend exactly 25 counties for heat-resilience research grants, to design a defensible risk-proportional $10 million allocation, and to quantify—through Jaccard overlap—how much the joint ranking differs from the heat-only and health-only rankings that a less integrated process might have produced. Our guiding hypothesis is that the joint, population-weighted index identifies a set of priority counties that no single-axis ranking can reproduce, and that explicitly accounting for uncertainty is necessary to defend the resulting recommendations.

2 Materials and Methods

2.1 Study domain and geographic units

The analysis covers the contiguous United States, operationalized as the 48 conterminous states plus the District of Columbia (49 state-level jurisdictions). The unit of analysis is the county (or county-equivalent). We adopted the vintage of county boundaries used by the CDC PLACES 2024 release, which incorporates Connecticut's nine Planning Regions (FIPS 9,110–9,190) that replaced the state's eight legacy counties in 2022. After intersecting the two data sources, 3,109 counties had complete climate and health information and constitute the analytic sample. County Federal Information Processing Standard (FIPS) codes were retained as five-digit zero-padded strings throughout to prevent silent join errors.

2.2 Climate data and the compound heat-day metric

Daily maximum ($T_{\max}$) and minimum ($T_{\min}$) 2 m air temperature were obtained from Daymet version 4 R1, a 1 km gridded daily surface-weather product for North America produced by interpolation of quality-controlled ground station observations with comprehensive uncertainty quantification [28, 29]. For each of the 3,109 counties we queried the Daymet Single Pixel Extraction service at the county population centroid (from PLACES) for every day of the 30-year reference period 1991–2020, yielding a complete county $\times$ year matrix with no missing values (93,270 county-years). Daymet uses a 365-day calendar, dropping 31 December in leap years; counts are therefore expressed per calendar year. Three coastal or island centroids (Island, WA; Aransas, TX; Bay, FL) fell on water pixels and were snapped to the nearest land pixel by a small eastward longitude offset.

We define a *compound heat day* as a single calendar day on which

$$T_{\max} \geq 35\,^\circ\mathrm{C} \quad \text{and} \quad T_{\min} \geq 20\,^\circ\mathrm{C}, \tag{1}$$

i.e. an extreme daytime maximum (95 °F) co-occurring with a warm "tropical" night (68 °F) that impairs overnight physiological recovery [8, 9]. For each county we counted compound heat days in each year and took the 30-year mean, $\bar{H}_i$, as the county's baseline compound-heat exposure. This metric is deliberately more restrictive than a simple hot-day count: it isolates the day–night episodes most strongly associated with excess mortality [11, 12].

2.3 Health data and chronic-disease burden

Age-adjusted prevalence estimates for five heat-sensitive conditions in the adult (aged ≥18 years) population were drawn from the CDC PLACES 2024 county file (dataset identifier `d3i6-k6z5`): coronary heart disease (CHD), stroke, COPD, diagnosed diabetes, and any disability [30]. PLACES estimates are produced by a validated multilevel regression and poststratification (small-area estimation) model applied to Behavioral Risk Factor Surveillance System data, and are released with 95% confidence intervals that quantify model-based uncertainty [25, 26]. We also extracted the total adult population (P_i, `totalpop18plus`) and the county centroid coordinates. All 3,109 counties had complete values for every field.

2.4 Percentile transformation and the composite score

To place the climate and health axes on a common, distribution-free footing, each was converted to a national percentile. For a vector of county values x, the percentile is computed as the average rank divided by the number of counties, $\mathrm{pct}(x_i) = \mathrm{rank}(x_i)/n$ with ties assigned the mean rank. The *heat-burden percentile* $h_i^{\text{heat}} = \mathrm{pct}(\bar{H}_i)$ is the national percentile of a county's mean compound-heat exposure. The *health-burden percentile* is the mean of the five condition-specific percentiles,

$$h_i^{\text{health}} = \frac{1}{5}\sum_{c\in\mathcal{C}} \mathrm{pct}(y_{i,c}), \qquad \mathcal{C} = \{\text{CHD, stroke, COPD, diabetes, disability}\}, \tag{2}$$

where $y_{i,c}$ is the age-adjusted prevalence of condition c in county i. Averaging percentiles rather than raw prevalences prevents any single high-prevalence condition from dominating and keeps each condition on an equal footing. The *composite vulnerability score* multiplies the two percentile axes by the exposed adult population,

$$S_i = h_i^{\text{heat}} \times h_i^{\text{health}} \times P_i. \tag{3}$$

The multiplicative form encodes a policy judgement that priority requires the *conjunction* of hazard, sensitivity, and scale: a county scores highly only if it is simultaneously hot, sick, and populous, and a near-zero value on any axis suppresses the score. Counties were ranked in descending order of S_i; the 25 highest-scoring counties constitute the recommended set.

2.5 Monte Carlo propagation of uncertainty

Point estimates conceal the substantial uncertainty in both inputs. We therefore propagated two independent sources of uncertainty through 1,000 Monte Carlo iterations (random seed 42 for full reproducibility), recomputing the entire national ranking in each iteration [27, 31].

Climate (interannual variability). In each iteration we resampled the 30 observed annual compound-heat counts for every county with replacement (a nonparametric bootstrap over years), recomputed the resampled 30-year mean, and re-derived the national heat-burden percentile. This preserves the empirical interannual distribution without assuming a parametric form and reflects the fact that a county's "typical" exposure is itself estimated from a finite record.

Health (small-area estimation uncertainty). For each county and condition we drew a prevalence value from a normal distribution centred on the PLACES point estimate with standard deviation $\sigma_{i,c} = (\mathrm{CI}^{\mathrm{high}}_{i,c} - \mathrm{CI}^{\mathrm{low}}_{i,c})/(2 \times 1.96)$ recovered from the reported 95% confidence interval, truncating draws to the physically valid range $[0, 100]\%$. The five draws were converted to percentiles and averaged as in Equation (2).

In every iteration the resampled heat and health percentiles were multiplied by the (fixed) adult population to give a simulated composite score, and all 3,109 counties were re-ranked. For each county we recorded the 5th, 50th, and 95th percentiles of its simulated rank (the 90% rank-stability interval), the median simulated composite score, and the probability of appearing in the top 25, $\Pr(\mathrm{rank} \leq 25)$. The full simulation completed in approximately 6 s.

2.6 Risk-proportional grant allocation

To translate the ranking into a funding recommendation we distributed a fixed \$10 million research budget across the 25 recommended counties in proportion to composite score,

$$A_i = B \times \frac{S_i}{\sum_{j \in \text{Top-25}} S_j}, \qquad B = 10{,}000{,}000\,\$, \tag{4}$$

so that allocations sum exactly to the budget. As a robustness check we computed a parallel allocation proportional to the *median simulated* composite score from the Monte Carlo, which down-weights counties whose high baseline score depends on a fragile input configuration.

2.7 Comparison with single-axis rankings

To test whether the joint index is redundant with simpler schemes, we constructed four alternative top-25 sets and compared each with the composite set using the Jaccard similarity coefficient, $J(A, B) = |A \cap B|/|A \cup B|$. The alternatives were: heat-only intensity (rank by h^{heat}_i), heat-only population-weighted ($h^{\mathrm{heat}}_i \times P_i$), health-only intensity (rank by h^{health}_i), and health-only population-weighted ($h^{\mathrm{health}}_i \times P_i$). We also computed the full pairwise Jaccard matrix across all five schemes. A low Jaccard value indicates that the joint index selects counties that the corresponding single-axis ranking would miss.

2.8 Software and reproducibility

All computations used Python with `NumPy`, `pandas`, and `SciPy`; choropleth maps were rendered with `GeoPandas` and `Matplotlib` using U.S. Census cartographic boundary files (2024 vintage) reprojected to the USA Contiguous Albers Equal Area Conic projection (EPSG:5070) for area-faithful display. The pipeline is deterministic given the fixed random seed, and all intermediate tables are archived to support independent replication.

3 Results

3.1 National geography of compound heat and chronic-disease burden

Compound heat days are sharply concentrated in the South and Southwest (Figure 1). Across all county-years the mean count is 8.1 days per year (median 2.3), but the distribution is extremely right-skewed: 364 counties, mostly in the northern tier of Montana, the upper Midwest, and interior New York and New England, never experienced a single compound heat day over the entire 30-year record, whereas the hottest counties averaged well over 100 per year. Imperial (CA) tops the exposure distribution at 120.6 compound days annually, followed by Maricopa (AZ, 114.5), La Paz (AZ), Zapata (TX), and Yuma (AZ). The pattern traces the low-elevation deserts of the Southwest, the Central Valley of California, and the humid subtropical belt of Texas and the Gulf Coast, where both extreme maxima and warm, humid nights are common. This spatial signature is physically coherent and consistent with the climatology of dangerous heat in the United States [3, 5].

The chronic-disease burden follows a different and largely independent geography (Figure 2). The highest health-burden percentiles form the familiar diagonal band running from the Lower Mississippi Delta and the Deep South through Appalachia and into the industrial Midwest and Rust Belt, together with pockets of the desert Southwest with large Native American populations and parts of south Texas. Much of the intermountain West, the northern Great Plains, and the affluent coastal counties of the Northeast and Pacific coast sit in the lower health-burden percentiles. The modest positive correlation between the heat-burden and health-burden percentiles across all counties ($r = 0.41$) confirms that the two axes are related—the Deep South is both hot and unhealthy—but are far from interchangeable, which is the essential precondition for a joint index to add information beyond either axis alone.

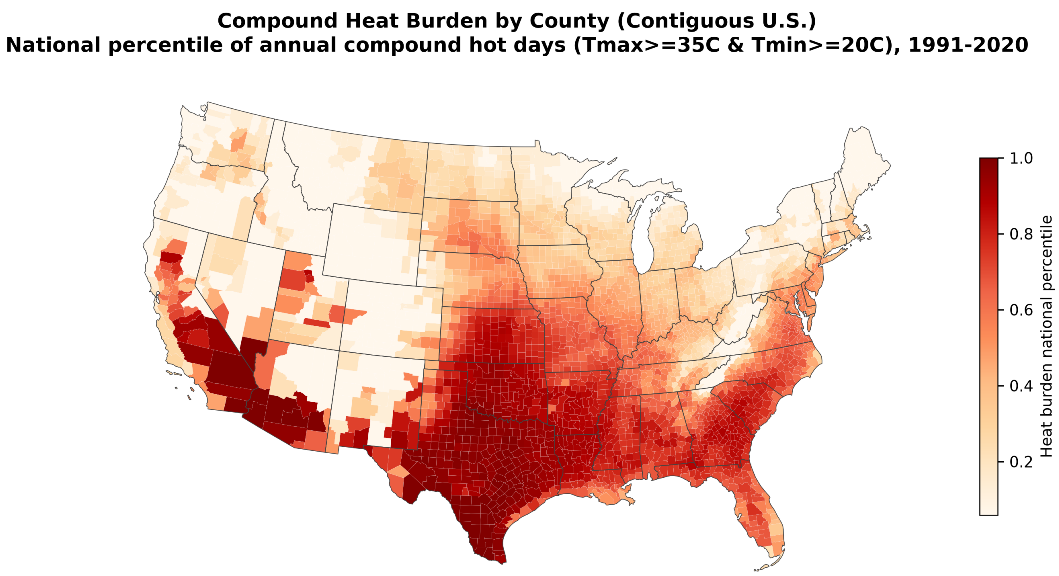

Figure 1. Compound heat burden by county. National percentile of the 30-year (1991–2020) mean annual count of compound heat days, defined as calendar days with $T_{\max} \geq 35\,^{\circ}\mathrm{C}$ *and* $T_{\min} \geq 20\,^{\circ}\mathrm{C}$ (Daymet V4 R1). Darker reds indicate higher percentiles. Exposure is concentrated in the desert Southwest, the California Central Valley, and the Texas–Gulf Coast humid subtropics; 364 northern-tier counties recorded no compound heat days. Albers equal-area projection (EPSG:5070).

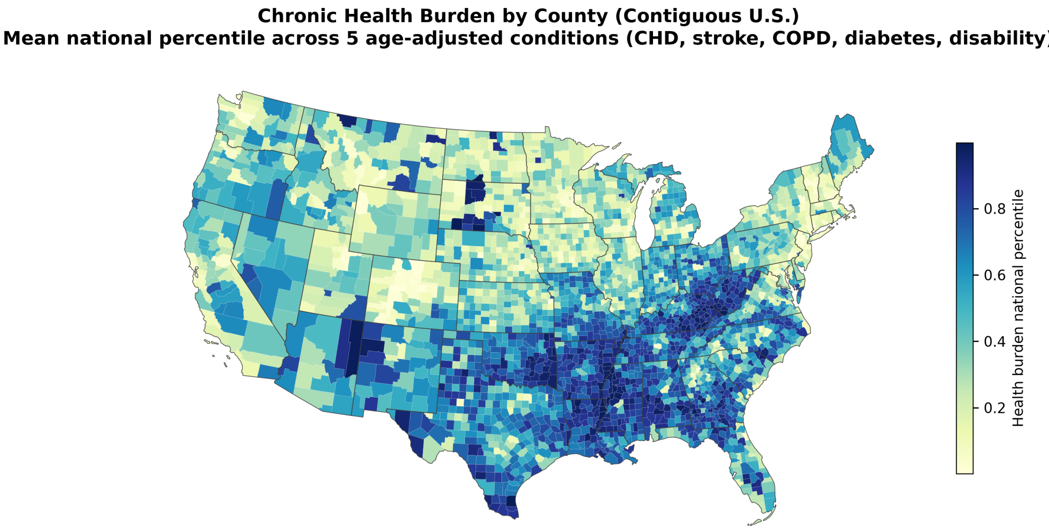

Figure 2. Chronic health burden by county. Mean national percentile across five age-adjusted conditions (coronary heart disease, stroke, COPD, diabetes, and disability) from CDC PLACES 2024. Darker blues indicate higher combined burden. The highest-burden band runs through the Lower Mississippi Delta, the Deep South, Appalachia, and the industrial Midwest—a geography only partly coincident with that of compound heat.

3.2 The joint composite vulnerability surface and the recommended 25 counties

Multiplying the two percentile axes by adult population produces the composite vulnerability surface of Figure 3, whose score spans several orders of magnitude and is therefore displayed on a $\log_{10}$ scale. The highest composite values fall almost exclusively on large metropolitan counties of the Sun Belt, where all three ingredients—hazard, sensitivity, and scale—are simultaneously large. The 25 recommended counties, outlined in the figure, are listed in full in Table 1. They are dominated by Texas (6 counties), California (5), and Florida (5), with Arizona, Nevada, Oklahoma (2), Tennessee, and—notably—Pennsylvania, New York, Illinois, and Michigan also represented. Twenty-one of the 25 lie in Southern or Southwestern Sun Belt states. Together the recommended counties contain 43,621,450 adults, approximately 16.8 % of the contiguous-U.S. adult population, underscoring that the joint index directs attention toward places where the aggregate number of at-risk residents is very large.

Harris County, Texas (Houston) ranks first by a wide margin, combining a very high compound-heat percentile (0.94), an elevated health-burden percentile (0.62), and the second-largest adult population in the set (3,550,425). Maricopa (Phoenix), Dallas, Los Angeles, and Bexar (San Antonio) complete the top five. Inspection of Table 1 reveals the value of the multiplicative design: the set mixes counties that qualify through different combinations of the three factors. Some, such as Maricopa, Clark (Las Vegas), San Bernardino, and Riverside, enter chiefly through extreme heat (heat percentiles ≥ 0.95) paired with large populations, despite only moderate health burden. Others—Philadelphia, the Bronx, Cook (Chicago), and Wayne (Detroit)—are the four Northern industrial metros in the set; their compound-heat percentiles are only moderate (0.42–0.59), and they qualify through the conjunction of very large or high-health-burden populations with non-trivial heat. A third group, such as Hidalgo and El Paso in south Texas and Shelby (Memphis), combines high heat with high disease prevalence in mid-sized populations. This heterogeneity is exactly what a joint index is designed to surface and what a single-axis ranking would flatten.

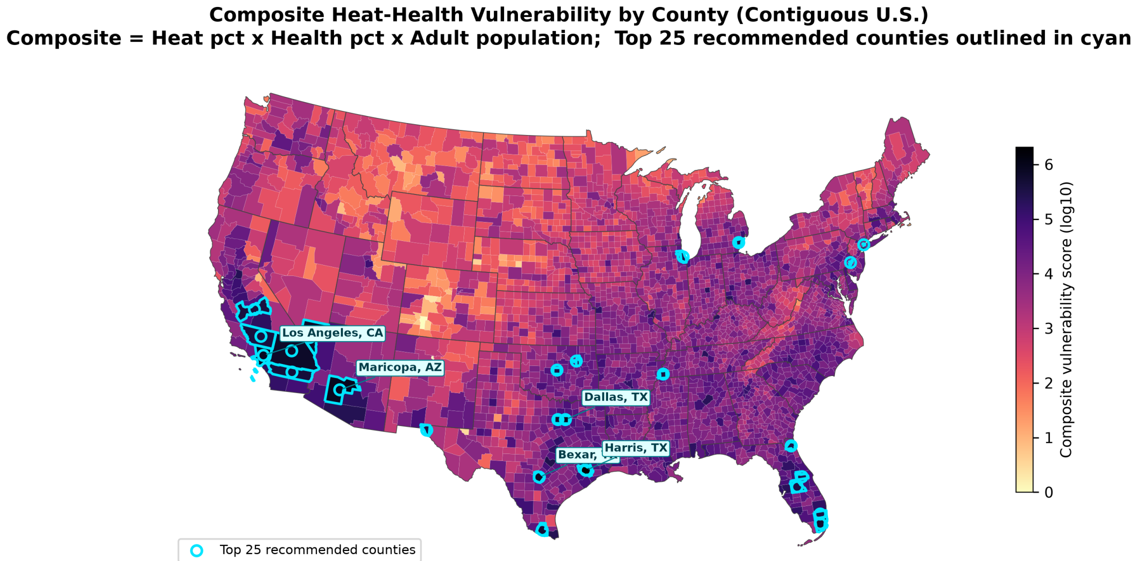

Figure 3. Composite heat–health vulnerability by county. $\log_{10}$ of the composite score $S_i = h_i^{\text{heat}} \times h_i^{\text{health}} \times P_i$. The 25 recommended counties are outlined in cyan with centroid markers; the top five are labelled. High composite vulnerability concentrates on large Sun Belt metropolitan counties where extreme compound heat, heavy chronic-disease burden, and large exposed populations coincide.

3.3 Rank stability under uncertainty

The Monte Carlo simulation shows that the recommended ranking is highly robust to plausible climatic and epidemiological uncertainty (Figure 4). Twenty-four of the 25 counties have a probability greater than 0.7 of remaining within the top 25 across the 1,000 simulations, and 23 exceed 0.9; the mean top-25 retention probability is 0.95. The five highest-ranked counties are effectively deterministic—Harris, Maricopa, Dallas, Los Angeles, and Bexar each remain in the top 25 in 100 % of iterations, with narrow 90% rank-stability intervals (for example, Harris occupies rank 1 in every iteration). As expected, the intervals widen toward the tail of the list, where composite scores are closely spaced and small input perturbations can reorder neighbouring counties. Orange (FL) and Tulsa (OK), ranked 24th and 25th, have the widest intervals and the lowest retention probabilities (0.72 and 0.41, respectively), indicating that membership at the very bottom of the recommended set is the least certain and could reasonably be contested by closely trailing counties. This graded confidence is precisely the information a funder needs: the top of the list can be treated as firm, while the marginal 25th slot warrants human judgement and possibly a sensitivity review.

Table 1. The 25 counties recommended for heat-resilience research funding. Counties are ordered by the baseline composite vulnerability score, defined as the product of the compound-heat national percentile (P_{heat}), the chronic-health-burden national percentile (P_{health}), and the adult (age ≥ 18) population. Adult population is given in thousands. The composite score is reported in units of 10^3 percentile-population. The 90 % rank interval spans the 5th–95th percentile of the simulated rank across 1,000 Monte Carlo iterations; P_{25} is the probability that a county falls within the top 25. The final column is the baseline risk-proportional share of the $10 million budget.

Rank	**County**	**St.**	**Adult pop.** (10^3)	P_{heat}	P_{health}	**Score** (10^3)	**90% rank interval**	P_{25}	**Award** ($M)
1	Harris	TX	3,550	0.94	0.62	2,077.3	1–1	1.000	1.47
2	Maricopa	AZ	3,532	1.00	0.26	909.1	2–5	1.000	0.64
3	Dallas	TX	1,953	0.98	0.46	880.8	2–5	1.000	0.62
4	Los Angeles	CA	7,737	0.52	0.21	860.0	2–6	1.000	0.61
5	Bexar	TX	1,553	0.99	0.50	774.4	4–7	1.000	0.55
6	Clark	NV	1,808	1.00	0.39	704.7	4–8	1.000	0.50
7	San Bernardino	CA	1,636	1.00	0.41	672.2	5–9	1.000	0.48
8	Tarrant	TX	1,611	0.99	0.38	601.4	6–11	1.000	0.43
9	Miami-Dade	FL	2,145	0.49	0.53	559.8	7–12	1.000	0.40
10	Philadelphia	PA	1,237	0.59	0.76	553.6	8–12	1.000	0.39
11	Hidalgo	TX	615	1.00	0.86	528.8	9–12	1.000	0.38
12	Riverside	CA	1,880	0.95	0.24	433.2	9–18	0.994	0.31
13	Kern	CA	656	0.95	0.64	398.8	12–19	1.000	0.28
14	Fresno	CA	735	0.92	0.58	392.1	12–20	0.998	0.28
15	Shelby	TN	688	0.81	0.68	377.7	13–21	1.000	0.27
16	Broward	FL	1,547	0.46	0.52	373.6	12–25	0.956	0.26
17	Bronx	NY	1,045	0.51	0.70	373.4	13–21	0.999	0.26
18	Cook	IL	4,040	0.46	0.19	351.6	12–27	0.926	0.25
19	Wayne	MI	1,345	0.42	0.60	340.2	15–25	0.961	0.24
20	Oklahoma	OK	602	0.92	0.61	335.8	16–26	0.948	0.24
21	Polk	FL	616	0.76	0.71	332.4	17–26	0.926	0.24
22	El Paso	TX	644	0.92	0.56	330.6	17–26	0.938	0.23
23	Duval	FL	791	0.74	0.57	330.4	17–26	0.908	0.23
24	Orange	FL	1,146	0.71	0.38	311.2	16–29	0.725	0.22
25	Tulsa	OK	510	0.90	0.64	295.6	22–29	0.411	0.21
Total			43,621						10.00

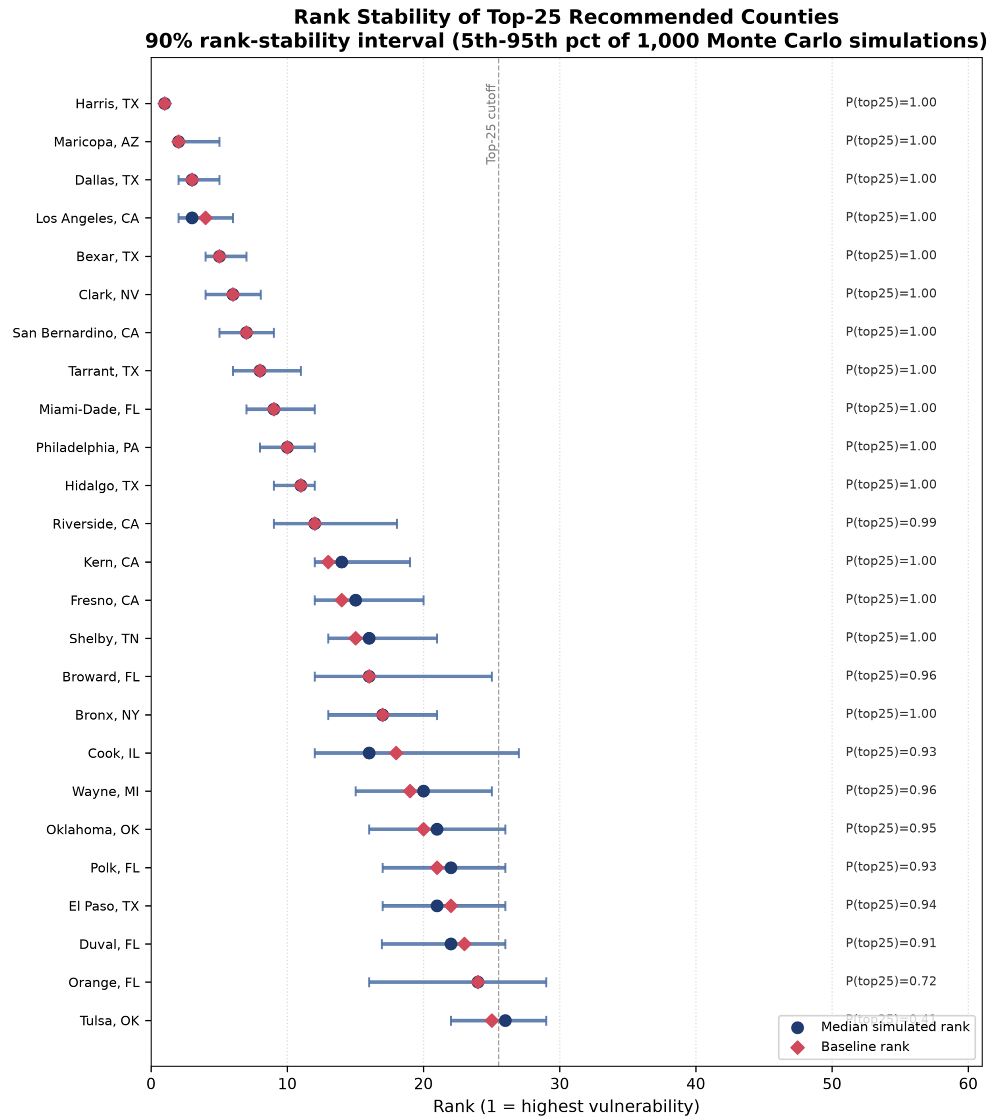

Figure 4. Rank-stability intervals for the recommended 25 counties. For each county the red diamond marks the baseline rank and the blue circle the median simulated rank; horizontal bars span the 90% rank-stability interval (5th–95th percentile of 1,000 Monte Carlo ranks). The annotation reports each county's probability of remaining in the top 25. Intervals are tight at the top of the list and widen toward the 25th position.

3.4 Risk-proportional funding allocation

Distributing the \$10 million budget in proportion to composite score yields the allocation shown in Figure 5 and tabulated in Table 1. Because the composite score is heavily right-skewed, the allocation is correspondingly concentrated: Harris County receives \$1.47 M (14.7 % of the budget), the top five counties together receive \$3.90 M (39.0 %), and awards decline smoothly to \$0.21 M for Tulsa (OK). The allocation derived from the median simulated composite score is virtually identical to the baseline allocation for almost every county—the two bars in Figure 5 are nearly indistinguishable—with per-county differences generally below \$0.03 M. The largest reallocations under the simulation-based scheme modestly *increase* awards to the very large, lower-heat metros whose composite scores are most stable (for example Maricopa, Los Angeles, and Cook), and slightly reduce awards to Harris; both allocations sum exactly to \$10 million by construction. The close agreement between the baseline and uncertainty-aware allocations is reassuring evidence that the funding recommendation is not an artefact of a single fragile point estimate.

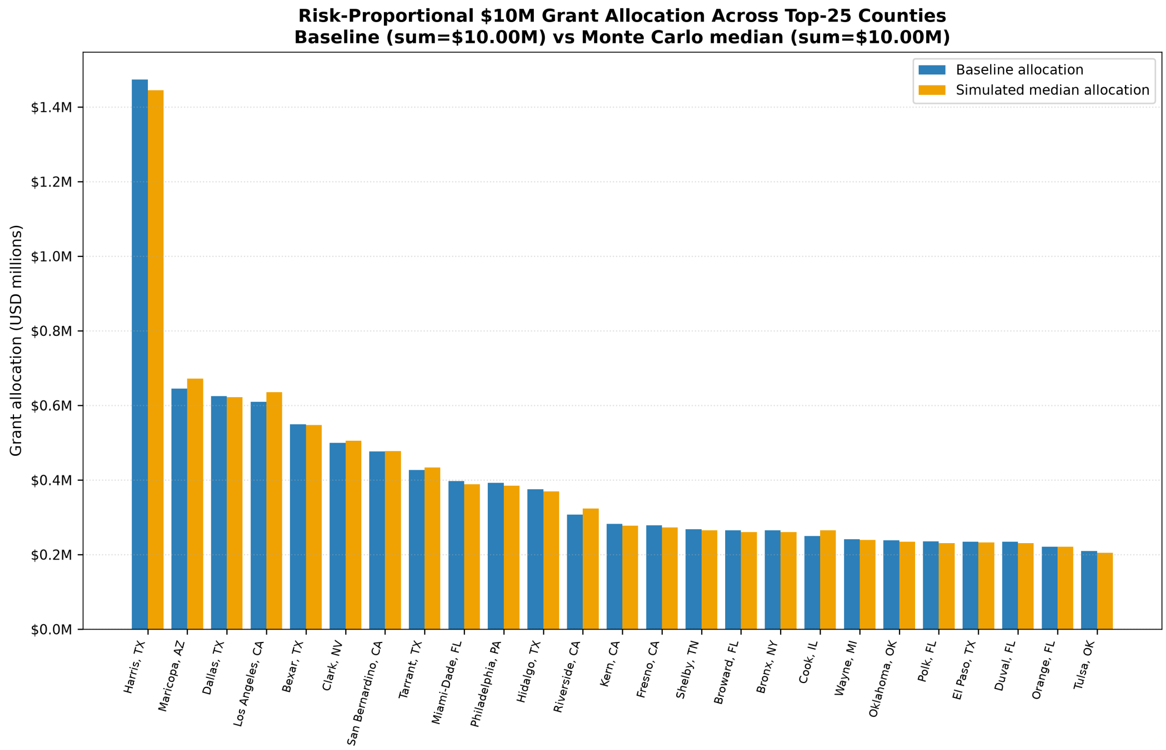

Figure 5. Risk-proportional \$10M grant allocation across the recommended 25 counties. Blue bars show the baseline allocation (proportional to the composite score); orange bars show the allocation proportional to the median simulated composite score. Both schemes sum exactly to \$10 million. The allocation is concentrated at the top of the list and the two schemes agree closely, indicating robustness of the funding recommendation to input uncertainty.

3.5 Discordance between the joint index and single-axis rankings

The comparison with single-axis rankings demonstrates that the joint index is not reproducible by any simpler scheme (Figure 6). A health-only intensity ranking—selecting the counties with the highest average disease-prevalence percentile irrespective of heat or population—shares *none* of its top 25 with the composite set ($J = 0.00$); such a ranking is dominated by small, rural, high-prevalence counties in the Deep South and Appalachia that experience little compound heat and house few people. A heat-only intensity ranking overlaps only slightly ($J = 0.09$; four counties in common), because the hottest counties by intensity are sparsely populated desert and south-Texas border counties. Population-weighting improves the overlap—the heat-only population-weighted ranking reaches $J = 0.39$ (14 counties in common) and the health-only population-weighted ranking reaches $J = 0.61$ (19 counties)—confirming that population scale is the single most influential factor, yet even the closest single-axis ranking still disagrees with the joint index on roughly a quarter to two-fifths of its members. The full pairwise structure in Figure 6 further shows that the two single-axis *intensity* rankings are almost entirely disjoint from one another ($J = 0.06$) and from every population-weighted scheme, reflecting the near independence of raw hazard intensity and raw disease intensity once population is set aside. In short, the joint, population-weighted composite occupies a distinct position in this space: it inherits the population sensitivity that both weighted schemes share while enforcing the simultaneous presence of hazard and sensitivity that neither single-axis scheme guarantees.

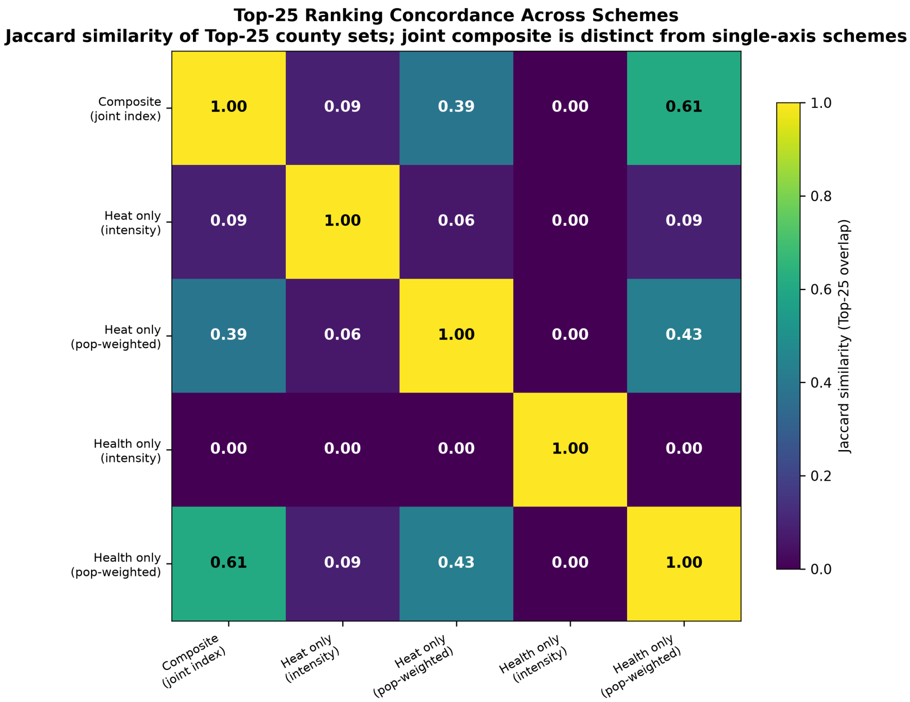

Figure 6. Top-25 concordance across ranking schemes. Jaccard similarity of the top-25 county sets selected by the joint composite index and four single-axis schemes. The composite set shares 0 % of members with a health-only intensity ranking, 9 % with a heat-only intensity ranking, 39 % with a heat-only population-weighted ranking, and 61 % with a health-only population-weighted ranking. No single-axis scheme reproduces the joint ranking.

4 Discussion

4.1 Principal findings

Applying a transparent, uncertainty-aware framework to three decades of daily temperature and the most recent national small-area health estimates, we identify 25 contiguous-U.S. counties whose residents face the greatest *joint* burden of compound heat exposure and heat-sensitive chronic disease at the largest population scale. The recommended set is strongly clustered in the South and Southwest, is led by the major Sun Belt metropolitan counties, and is highly stable to plausible perturbations of its climatic and epidemiological inputs. A risk-proportional \$10 million allocation follows directly and mechanically from the composite scores, and it is essentially unchanged when computed from uncertainty-adjusted rather than point-estimate scores. Most importantly, the joint ranking selects a portfolio of counties that no single-axis ranking—whether based on heat alone or health alone, with or without population weighting—can reproduce.

4.2 Interpretation of the spatial pattern

The concentration of joint vulnerability in the South and Southwest reflects the superposition of three overlapping but non-identical geographies. The compound-heat metric isolates the low-desert Southwest, the California Central Valley, and the humid Texas–Gulf Coast, where extreme daytime maxima are routinely accompanied by warm nights that foreclose recovery [8, 12]. The chronic-disease geography adds the Deep South, the Lower Mississippi Delta, and the industrial Midwest, where cardiometabolic and respiratory disease prevalence is highest [15]. Population weighting then pulls the joint ranking toward the large metropolitan cores—Houston, Phoenix, Dallas, Los Angeles, San Antonio, Las Vegas—where urban-heat-island amplification raises nighttime temperatures still further and where the built environment and legacies of residential segregation concentrate both exposure and social disadvantage [18, 20, 21]. The appearance of four Northern industrial metros (Philadelphia, the Bronx, Cook, Wayne) despite only moderate compound-heat exposure is instructive: their inclusion is driven by the combination of very large or high-health-burden populations with non-negligible heat, and it is a reminder that acclimatization is lower and heat-response infrastructure often weaker in cities that experience heat less frequently, a pattern implicated in the high death tolls of the 1995 Chicago and 2006 heat events [11, 32].

4.3 Why a joint, population-weighted index matters for funding

The Jaccard analysis makes the policy stakes concrete. Had the prioritization been conducted on health status alone, none of the resulting counties would have overlapped with the joint recommendation; the funding would have flowed to small, rural, high-prevalence counties where the absolute number of people exposed to dangerous compound heat is low. Had it been conducted on heat intensity alone, it would have targeted sparsely populated desert and border counties. Either single-axis choice would have been defensible in isolation yet would have misallocated resources relative to the goal of reducing aggregate, population-scale heat-health harm. The joint index resolves this by requiring the conjunction of hazard, sensitivity, and scale, and the multiplicative form ensures that a county cannot compensate for a near-absence of heat with extreme disease prevalence, or vice versa. This is consistent with the physiological reality that chronic disease is a risk *modifier* of heat rather than an independent cause of heat death: it matters most precisely where heat is severe and many people are exposed [14, 16]. For a programme officer, the practical implication is that the axis on which places are ranked is not a technical detail but a decisive determinant of who receives support.

4.4 The value of propagating uncertainty

Reporting rank-stability intervals and top-set membership probabilities, rather than a bare ordinal list, converts a brittle ranking into an actionable decision aid [27]. Our results show that the top of the list can be treated as firm—the leading counties retain their positions in every simulation—whereas the marginal 25th position is genuinely uncertain (Tulsa's top-25 probability is only 0.41). A defensible process would fund the high-probability counties without reservation, treat the low-probability tail as a watch-list subject to additional review, and disclose these probabilities to stakeholders. The near-identity of the baseline and simulation-based allocations further indicates that, for this particular budget rule, the point-estimate recommendation is not being propped up by a single fragile input. The general lesson—that composite indicators used for resource allocation should carry an explicit account of input uncertainty—applies well beyond heat and directly addresses a longstanding critique of vulnerability indices [23, 24].

4.5 Comparison with prior work

Our framework builds on and extends the substantial literature on heat-vulnerability indices [22–24]. It differs in three respects that we regard as consequential. First, most prior indices summarise the climate hazard with annual-mean temperature, a coarse heat-day count, or a single extreme-event exposure; our compound day–night metric is grounded in the physiology of overnight recovery and in the epidemiological evidence that hot nights independently elevate mortality [8, 9, 12]. Second, whereas most indices report deterministic scores, we propagate both interannual climate variability and the model-based uncertainty inherent in small-area disease estimates [25], delivering the rank-stability information that decision-makers require. Third, we close the loop from index to action by attaching a defensible, uncertainty-checked budget rule. The strong role of population scale that we find echoes national analyses linking extreme heat to cardiovascular and all-cause mortality at the county level [15, 17] and the recognition that the U.S. heat-health burden is concentrated in large, warming metropolitan areas [7, 33].

4.6 Limitations

Several limitations temper the interpretation of our results. First, county centroids are point locations, and the Daymet single-pixel extraction at a centroid does not capture within-county heterogeneity in exposure, including fine-scale urban-heat-island structure; a population-weighted areal aggregation of the full 1 km grid would refine the exposure estimate, particularly for large or topographically diverse counties. Second, the compound heat-day thresholds (35 °C and 20 °C) are physiologically motivated but nonetheless fixed and absolute; because acclimatization shifts the temperature–mortality relationship, an absolute threshold may understate the effective hazard in normally cool, poorly adapted regions and overstate it in chronically hot ones [6, 32]. Third, humidity is not represented explicitly; heat stress depends on the combination of temperature and moisture, and a wet-bulb or heat-index formulation would better capture the Gulf Coast in particular. Fourth, PLACES prevalences are model-based small-area estimates rather than direct measurements, and although we propagate their reported confidence intervals, any systematic bias in the underlying model would propagate as well [25, 26]. Fifth, the five chronic conditions are weighted equally and are not exhaustive; kidney disease, mental illness, and substance use also modify heat risk, and the equal-weight choice, while transparent, is a value judgement. Sixth, our health-burden axis captures the prevalence of sensitivity but not adaptive capacity—air-conditioning penetration, cooling-centre access, tree canopy, and social isolation—which a fuller vulnerability assessment would incorporate [19, 23]. Finally, the composite is a relative prioritization tool, not an estimate of attributable deaths; it ranks where joint burden is greatest but does not by itself quantify the health gains expected from a given intervention.

4.7 Policy implications and future directions

Notwithstanding these limitations, the framework offers programme officers a defensible, transparent, and reproducible basis for geographically targeting heat-resilience research investments. Its outputs—a ranked county list, rank-stability intervals, membership probabilities, and a risk-proportional budget—map directly onto the decisions a funder must make. Natural extensions include replacing the single-pixel exposure with a population-weighted areal grid, substituting a humidity-aware heat metric such as wet-bulb globe temperature, incorporating an explicit adaptive-capacity axis, and coupling the index to downscaled climate projections so that priorities reflect not only historical but future compound-heat burden [4, 12, 33]. Because every step is scripted and every input is public, the framework can be re-run annually as PLACES and Daymet are updated, and its thresholds and weights can be adjusted to reflect a funder's explicit priorities and audited by stakeholders.

5 Conclusion

Dangerous heat is a compound, day–night phenomenon whose lethality is governed jointly by the severity of the climatological hazard, the chronic-disease burden of the exposed population, and the number of people at risk. Ranking places along any single one of these axes—as much research- and adaptation-funding practice implicitly does—produces recommendations that a joint analysis shows to be substantially misdirected. By integrating a physiologically grounded compound-heat metric from Daymet with five age-adjusted chronic-disease prevalences from CDC PLACES, weighting by adult population, and propagating both climatic and epidemiological uncertainty through a Monte Carlo simulation, we identify 25 contiguous-U.S. counties—overwhelmingly large Sun Belt metropolitan areas led by Harris, Maricopa, Dallas, Los Angeles, and Bexar—that jointly bear the greatest heat-health burden. The ranking is stable, the resulting risk-proportional $10 million allocation is robust to input uncertainty, and the selected portfolio is not reproducible by any heat-only or health-only ranking. We recommend that heat-resilience research grants be allocated on the basis of joint, population-weighted, uncertainty-aware vulnerability, and we provide both the shortlist and the fully reproducible machinery to support and revisit that decision.

Data and Code Availability

Daymet V4 R1 daily temperature data are available from the ORNL DAAC (`https://doi.org/10.3334/ORNLDAAC/2129`). The CDC PLACES 2024 County dataset (identifier `d3i6-k6z5`) is available from `https://data.cdc.gov`. County boundary files are the U.S. Census Bureau 2024 cartographic boundary files. All derived tables (full county rankings, the top-25 recommendations, the Jaccard matrix, and the annual compound-heat counts) and the analysis scripts underlying every figure and result reported here are archived in the project repository to support independent replication.

Acknowledgements

This analysis relies on the public data infrastructure maintained by the Oak Ridge National Laboratory Distributed Active Archive Center and the U.S. Centers for Disease Control and Prevention. No external funding supported this work.

References

[1] Ambarish Vaidyanathan, Josephine Malilay, Paul Schramm, and Shubhayu Saha. Heat-related deaths — United States, 2004–2018. *Morbidity and Mortality Weekly Report (MMWR)*, 69(24):729–734, 2020. doi: 10.15585/mmwr.mm6924a1.

[2] Kristie L. Ebi, Anthony Capon, Peter Berry, Carolyn Broderick, Richard de Dear, George Havenith, Yasushi Honda, R. Sari Kovats, Wei Ma, Arunima Malik, Nathan B. Morris, Lars Nybo, Sonia I.

Seneviratne, Jennifer Vanos, and Ollie Jay. Hot weather and heat extremes: health risks. *The Lancet*, 398(10301):698–708, 2021. doi: 10.1016/S0140-6736(21)01208-3.

[3] Gerald A. Meehl and Claudia Tebaldi. More intense, more frequent, and longer lasting heat waves in the 21st century. *Science*, 305(5686):994–997, 2004. doi: 10.1126/science.1098704.

[4] Sonia I. Seneviratne, Xuebin Zhang, M. Adnan, W. Badi, C. Dereczynski, A. Di Luca, S. Ghosh, I. Iskandar, J. Kossin, S. Lewis, F. Otto, I. Pinto, M. Satoh, S. M. Vicente-Serrano, M. Wehner, and B. Zhou. Weather and climate extreme events in a changing climate. In *Climate Change 2021: The Physical Science Basis. Contribution of Working Group I to the Sixth Assessment Report of the Intergovernmental Panel on Climate Change*, pages 1513–1766. Cambridge University Press, Cambridge, United Kingdom and New York, NY, USA, 2021. doi: 10.1017/9781009157896.013.

[5] Dana Habeeb, Jason Vargo, and Brian Stone. Rising heat wave trends in large US cities. *Natural Hazards*, 76(3):1651–1665, 2015. doi: 10.1007/s11069-014-1563-z.

[6] Antonio Gasparrini, Yuming Guo, Masahiro Hashizume, Eric Lavigne, Antonella Zanobetti, Joel Schwartz, Aurelio Tobias, Shilu Tong, Joacim Rocklöv, Bertil Forsberg, et al. Mortality risk attributable to high and low ambient temperature: a multicountry observational study. *The Lancet*, 386(9991):369–375, 2015. doi: 10.1016/S0140-6736(14)62114-0.

[7] Michelle L. Bell, Antonio Gasparrini, and Georges C. Benjamin. Climate change, extreme heat, and health. *New England Journal of Medicine*, 390(19):1793–1801, 2024. doi: 10.1056/NEJMra2210769.

[8] Peninah Murage, Shakoor Hajat, and R. Sari Kovats. Effect of night-time temperatures on cause and age-specific mortality in London. *Environmental Epidemiology*, 1(2):e005, 2017. doi: 10.1097/EE9.0000000000000005.

[9] Dominic Royé. The effects of hot nights on mortality in Barcelona, Spain. *International Journal of Biometeorology*, 61(12):2127–2140, 2017. doi: 10.1007/s00484-017-1416-z.

[10] Karine Laaidi, Abdelkrim Zeghnoun, Bénédicte Dousset, Philippe Bretin, Stéphanie Vandentorren, Emmanuel Giraudet, and Pascal Beaudeau. The impact of heat islands on mortality in Paris during the August 2003 heat wave. *Environmental Health Perspectives*, 120(2):254–259, 2012. doi: 10.1289/ehp.1103532.

[11] Jan C. Semenza, Carol H. Rubin, Kenneth H. Falter, Joel D. Selanikio, W. Dana Flanders, Holly L. Howe, and John L. Wilhelm. Heat-related deaths during the July 1995 heat wave in Chicago. *New England Journal of Medicine*, 335(2):84–90, 1996. doi: 10.1056/NEJM199607113350203.

[12] Cheng He, Ho Kim, Masahiro Hashizume, Whanhee Lee, Yasushi Honda, Soo-Eun Kim, Patrick L. Kinney, Alexandra Schneider, Yali Zhang, Yixiang Zhu, Renjie Chen, and Haidong Kan. The effects of night-time warming on mortality burden under future climate change scenarios: a modelling study. *The Lancet Planetary Health*, 6(8):e648–e657, 2022. doi: 10.1016/S2542-5196(22)00139-5.

[13] Marcus C. Sarofim, Shubhayu Saha, Michael D. Hawkins, David M. Mills, Jeremy Hess, Radley Horton, Patrick Kinney, Joel Schwartz, and Alexis St. Juliana. Temperature-related death and illness. *The Impacts of Climate Change on Human Health in the United States: A Scientific Assessment. U.S. Global Change Research Program*, pages 43–68, 2016. doi: 10.7930/J0MG7MDX.

[14] Glen P. Kenny, Jane Yardley, Candice Brown, Ronald J. Sigal, and Ollie Jay. Heat stress in older individuals and patients with common chronic diseases. *Canadian Medical Association Journal*, 182 (10):1053–1060, 2010. doi: 10.1503/cmaj.081050.

[15] Sameed Ahmed M. Khatana, Rachel M. Werner, and Peter W. Groeneveld. Association of extreme heat and cardiovascular mortality in the United States: a county-level longitudinal analysis from 2008 to 2017. *Circulation*, 146(3):249–261, 2022. doi: 10.1161/CIRCULATIONAHA.122.060746.

[16] Aditi Bunker, Jan Wildenhain, Alina Vandenbergh, Nicholas Henschke, Joacim Rocklöv, Shakoor Hajat, and Rainer Sauerborn. Effects of air temperature on climate-sensitive mortality and morbidity outcomes in the elderly; a systematic review and meta-analysis of epidemiological evidence. *EBioMedicine*, 6:258–268, 2016. doi: 10.1016/j.ebiom.2016.02.034.

[17] Sameed Ahmed M. Khatana, Lauren A. Eberly, Ashwin S. Nathan, and Peter W. Groeneveld. Association of extreme heat with all-cause mortality in the contiguous US, 2008–2017. *JAMA Network Open*, 5(5):e2212957, 2022. doi: 10.1001/jamanetworkopen.2022.12957.

[18] Angel Hsu, Glenn Sheriff, Tirthankar Chakraborty, and Diego Manya. Disproportionate exposure to urban heat island intensity across major US cities. *Nature Communications*, 12(1):2721, 2021. doi: 10.1038/s41467-021-22799-5.

[19] Sharon L. Harlan, Anthony J. Brazel, Lela Prashad, William L. Stefanov, and Larissa Larsen. Neighborhood microclimates and vulnerability to heat stress. *Social Science & Medicine*, 63(11):2847–2863, 2006. doi: 10.1016/j.socscimed.2006.07.030.

[20] Jeremy S. Hoffman, Vivek Shandas, and Nicholas Pendleton. The effects of historical housing policies on resident exposure to intra-urban heat: a study of 108 US urban areas. *Climate*, 8(1):12, 2020. doi: 10.3390/cli8010012.

[21] Susanne A. Benz and Jennifer A. Burney. Widespread race and class disparities in surface urban heat extremes across the United States. *Earth's Future*, 9(7):e2021EF002016, 2021. doi: 10.1029/2021EF002016.

[22] Carina J. Gronlund. Racial and socioeconomic disparities in heat-related health effects and their mechanisms: a review. *Current Epidemiology Reports*, 1(3):165–173, 2014. doi: 10.1007/s40471-014-0014-4.

[23] Colleen E. Reid, Marie S. O'Neill, Carina J. Gronlund, Shannon J. Brines, Daniel G. Brown, Ana V. Diez-Roux, and Joel Schwartz. Mapping community determinants of heat vulnerability. *Environmental Health Perspectives*, 117(11):1730–1736, 2009. doi: 10.1289/ehp.0900683.

[24] Susan L. Cutter, Bryan J. Boruff, and W. Lynn Shirley. Social vulnerability to environmental hazards. *Social Science Quarterly*, 84(2):242–261, 2003. doi: 10.1111/1540-6237.8402002.

[25] Xingyou Zhang, James B. Holt, Hua Lu, Anne G. Wheaton, Earl S. Ford, Kurt J. Greenlund, and Janet B. Croft. Multilevel regression and poststratification for small-area estimation of population health outcomes: a case study of chronic obstructive pulmonary disease prevalence using the Behavioral Risk Factor Surveillance System. *American Journal of Epidemiology*, 179(8):1025–1033, 2014. doi: 10.1093/aje/kwu018.

[26] Xingyou Zhang, James B. Holt, Shumei Yun, Hua Lu, Kurt J. Greenlund, and Janet B. Croft. Validation of multilevel regression and poststratification methodology for small-area estimation of health indicators from the Behavioral Risk Factor Surveillance System. *American Journal of Epidemiology*, 182(2):127–137, 2015. doi: 10.1093/aje/kwv002.

[27] Michaela Saisana, Andrea Saltelli, and Stefano Tarantola. Uncertainty and sensitivity analysis techniques as tools for the quality assessment of composite indicators. *Journal of the Royal Statistical Society: Series A (Statistics in Society)*, 168(2):307–323, 2005. doi: 10.1111/j.1467-985X.2005.00350.x.

[28] Michele M. Thornton, Rupesh Shrestha, Yaxing Wei, Peter E. Thornton, Shih-Chieh Kao, and Bruce E. Wilson. Gridded daily weather data for North America with comprehensive uncertainty quantification. *Scientific Data*, 8(1):190, 2021. doi: 10.1038/s41597-021-00973-0.

[29] M. M. Thornton, R. Shrestha, Y. Wei, P. E. Thornton, and S.-C. Kao. Daymet: Daily surface weather data on a 1-km grid for North America, version 4 r1. ORNL Distributed Active Archive Center (ORNL DAAC), Oak Ridge, Tennessee, USA, 2022.

[30] Centers for Disease Control and Prevention. PLACES: Local data for better health, county data 2024 release. National Center for Chronic Disease Prevention and Health Promotion, Division of Population Health. Dataset identifier d3i6-k6z5, 2024. Available at `https://data.cdc.gov/500-Cities-Places/PLACES-Local-Data-for-Better-Health-County-Data-2024-release/d3i6-k6z5`.

[31] Bradley Efron. Bootstrap methods: another look at the jackknife. *The Annals of Statistics*, 7(1):1–26, 1979. doi: 10.1214/aos/1176344552.

[32] G. Brooke Anderson and Michelle L. Bell. Heat waves in the United States: mortality risk during heat waves and effect modification by heat wave characteristics in 43 U.S. communities. *Environmental Health Perspectives*, 119(2):210–218, 2011. doi: 10.1289/ehp.1002313.

[33] Kate R. Weinberger, Antonella Zanobetti, Joel Schwartz, and Gregory A. Wellenius. Projected temperature-related deaths in ten large U.S. metropolitan areas under different climate change scenarios. *Environment International*, 136:105320, 2020. doi: 10.1016/j.envint.2019.105320.